Artificial and Natural Excitation Testing of SWiFT Vestas V27 Wind Turbines

Timothy Marinone and David Cloutier
ATA Engineering, San Diego, CA, 92130

Bruce LeBlanc
Sandia National Laboratories,[1] Albuquerque, NM, 87185

Thomas Carne
MannaTech Engineering, Bozeman, MT, 59715

Palle Andersen
Structural Vibration Solutions A/S, Denmark

ABSTRACT

The Scaled Wind Farm Technology facility has been developed by Sandia National Laboratories to enable rapid, cost-efficient testing and development of transformative wind energy technology. As part of this effort, ATA Engineering was contracted by Sandia to perform modal testing on multiple fully assembled wind turbines to gain a better understanding of the structures.

This paper presents the results obtained from experimental modal analysis and operational modal analysis performed on Vestas V27 wind turbines recently installed at the Scaled Wind Farm Technology facility. Experimental modal results are compared between two identical wind turbines, identifying variability in both components and boundary conditions. Additionally, operational modal analysis was used on a single parked wind turbine under natural wind excitation. The operational modal results compare well to the results obtained from a conventional impact modal survey, providing promising results for future testing on larger turbines where measured external excitation may not be feasible.

Keywords: wind turbines, operational modal analysis, Stochastic Subspace Identification, experimental modal characterization, modal parameter estimation

INTRODUCTION

Sandia National Laboratories (SNL) is developing the Scaled Wind Farm Technology (SWiFT) facility to enable rapid, cost-efficient testing and development of transformative wind energy technology. The site is intended to study complex turbine wake interactions and focus on damage mitigation, improved power performance, and recommended future site layouts. Since this site is designed to be open source and to provide data to all interested parties, the models must be accurate enough to be used for the desired analyses while preserving Vestas' proprietary information. For this paper, two Vestas V27 (V27) wind turbines installed on site were tested to obtain modal properties for the validation of analysis models.

Experimental modal analysis (EMA) was performed on several components and two fully assembled SWiFT Vestas V27 wind turbines. In addition to modal testing performed on the full turbines, operational modal analysis (OMA) was performed on a turbine with the blades parked, using the wind as a source of natural excitation. While

---

[1] Sandia is a multiprogram laboratory operated by Sandia Corporation, a Lockheed Martin Company, for the U.S. Department of Energy under Contract DE-AC04-94AL85000.

the SWiFT V27 turbines are of a size where reasonable excitation can be imparted to the structure using a modal impact sledge, determining OMA limitations with respect to EMA provides greater insight for future testing of larger turbines. During construction and assembly of the wind farm, ATA Engineering, Inc., (ATA) was contracted to perform modal testing on the blades, hubs, nacelles, and towers in the free-free configuration and installed on the concrete foundations, as well as two fully assembled turbines. As instrumentation was already installed from the modal survey, time histories were recorded with rotors locked during periods of higher wind when modal testing could not be performed. These time histories were used in Structural Vibration Solutions' Ambient Response Testing and Modal Identifcation (ARTeMIS) Modal software to extract modal parameters for comparison to the experimental modal results.

The use of natural excitation to extract modal parameters has been shown to be a valid approach for many large structures. The natural excitation technique (NExT) was initially conceived in the 1980s for use on wind turbines. NExT has been successfully performed on several vertical axis wind turbines [1, 2] and shown to be a valid alternative to experimental modal analysis; both Polyreference and Eigensystem Realization algorithms were used as time-domain modal identification on auto- and cross-correlation functions computed from measured time histories.

Further development in OMA has led to additional techniques for use in civil, aerospace, and the automotive industries, where traditional modal testing may be impractical or too expensive. Frequency Domain Decomposition (FDD) [3, 4] and Stochastic Subspace Identification (SSI) are two common algorithms for extracting modal parameters. Both techniques have additional variations for improving modal extraction. In general, FDD uses a singular value decomposition of the power spectral density, in which the mode shapes are estimated as the singular vectors at each peak. SSI is a more sophisticated time-domain algorithm using a linear least-squares estimation of the model; with this approach, the full measured time histories are used. The limiting constraint with all techniques is the assumption that the test article is excited by steady-state random white noise across the frequency band of interest, which is a valid assumption in the case of a parked wind turbine.

TEST ARTICLE AND DATA COLLECTION

Three Vestas V27 225 kW wind turbines were recently installed at the Sandia National Laboratories (SNL) Scaled Wind Farm Technology (SWiFT) facility hosted at Texas Tech University in Lubbock, Texas. The turbines are heavily instrumented and modified variable-speed, variable-pitch V27 turbines. The two turbines shown in the middle and right side of Figure 1 are funded by the Department of Energy's Office of Energy Efficiency and Renewable Energy and are named SNL1 and SNL2, with SNL1 located on the right. The third turbine, shown in the left of Figure 1, was installed by Vestas R&D of Houston.

Figure 1. SWiFT Vestas V27 wind farm at Texas Tech University in Lubbock, Texas.

The SNL1 turbine was fully instrumented with eighty PCB T333B modal accelerometers installed on the blades, hub, nacelle, and tower, in addition to six seismic accelerometers on the foundation. Figure 2 shows the test display model with instrumentation locations. All accelerometers installed on the tower, nacelle, and hub were installed internally and could be accessed by the ladder mounted to the tower. Accelerometers installed externally on the blades could only be accessed by aerial lift. Both experimental modal analysis and operational modal analysis was performed on SNL1.

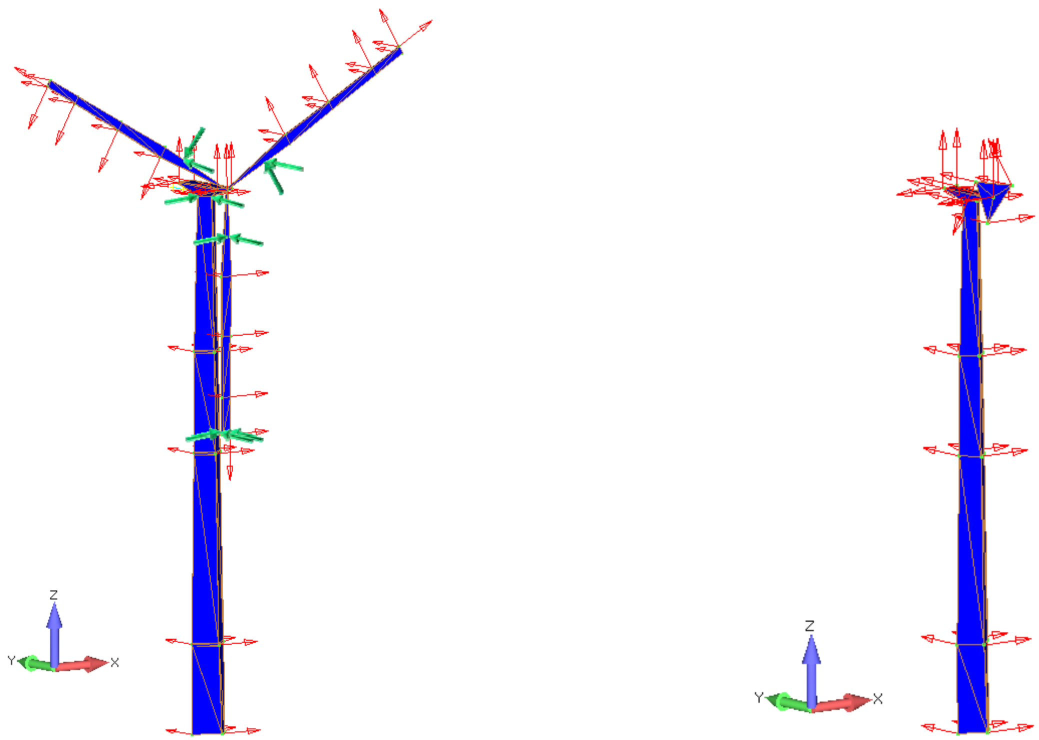

Figure 2. Test display models for SNL1 (left) and SNL2 (right). Green arrows represent excitation locations.

Due to high winds and limited test time, on SNL2 a reduced set of instrumentation was installed and only experimental modal testing was performed. This reduced set included forty-one accelerometers installed in the tower, nacelle, and hub, which matched locations on SNL1, and single biaxial accelerometers on each blade located near the maximum chord location, as shown in the right of Figure 2.

The wind speed significantly increased from morning to afternoon, so modal testing was limited to the early morning to reduce the effects of unmeasured excitation. Impact modal testing was performed with a modal sledge at locations indicated by the green arrows in Figure 2. Approximately six to eight averages were acquired at each impact location, using a sampling frequency of 80 Hz and a block size of 2056. Figure 3 shows a picture of the modal test being performed on SNL1.

Figure 3. Impact modal testing performed on SNL1.

Operational data was collected at 80 Hz for approximately two hours, with wind speeds around 14 m/s. The rotors were yawed approximately parallel to the wind direction, with the blades pitched to zero degrees. This configuration provided adequate excitation to the blades in both the edgewise and flapwise directions, as the flapwise modes are in general more easily excited.

TEST RESULTS

While the modal testing was performed early in the mornings to minimize the unmeasured excitation to the structure from the wind, a noticeable amount of excitation was still present at the low wind speeds of approximately 4 m/s. However, in spite of the unmeasured excitation, the overall coherence levels were still high for the majority of rotor accelerometers. Figure 4 presents the drive point frequency response function (FRF) and coherence overlay for excitation at the blade tip of SNL1 (indicated in Figure 2), showing good coherence across the frequency band of interest.

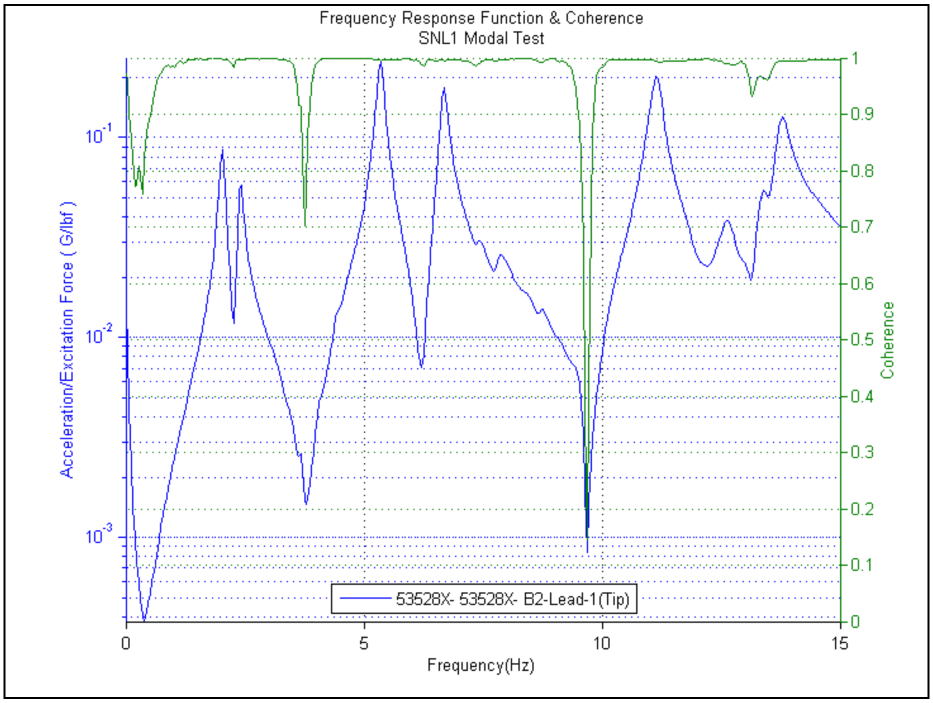

Figure 4. Drive point FRF and coherence from impact on SNL1 blade tip.

ATA Engineering's AFPoly™ was used to extract modal parameters from the impact modal survey. Twenty modes were extracted in the 0–15 Hz frequency band. The synthesized power spectrum mode-indicator function (PSMIF) in Figure 5 shows an overall good fit of the modal parameters. A test-analysis model (TAM) was made for back-expansion of the mode shapes for better visualization, providing an estimation of shape information to missing DOF; the back-expanded first three blade flapwise bending modes are shown in Figure 6.

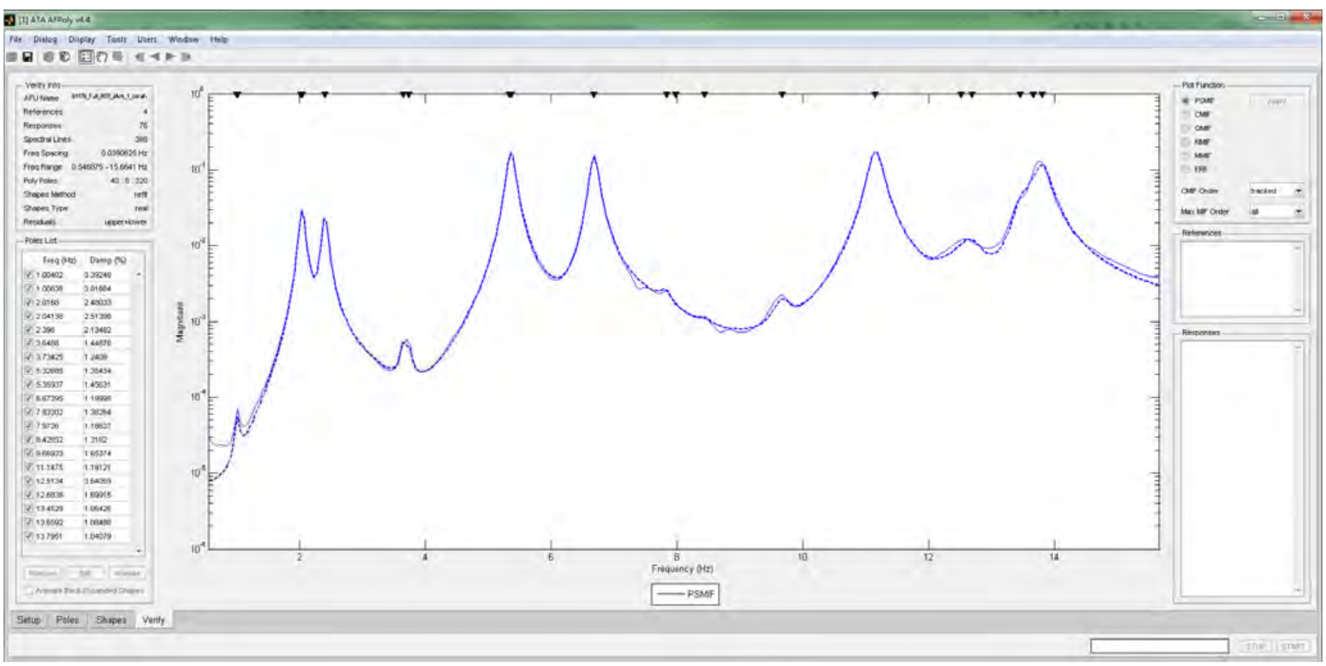

Figure 5. PSMIF overlay from fitted modal parameters.

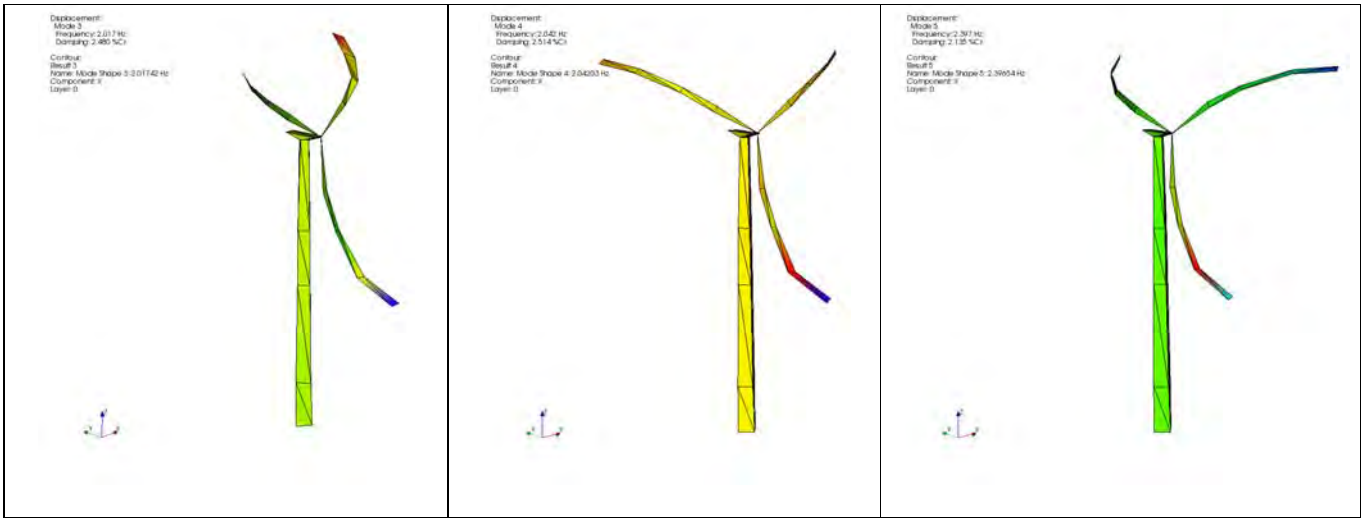

Figure 6. First three flapwise bending modes.

As the modal survey on SNL2 had a significantly reduced sensor set on the rotors, not all modes in the 0–15 Hz range could be easily identified. To compare modes between SNL1 and SNL2, a combination of frequency, MAC at the reduced sensor set, and comparing PSMIFs at the reduced sensor set were all used. Also, not all modes could be extracted or verified to correlate between the two turbines. The final comparison of modes between SNL1 and SNL2 is given in Table 1. An average of less than 2% frequency difference exists across all matched modes.

Table 1. Mode comparison between SNL1 and SNL2.

	SNL1		SNL2				
Mode	Frequency (Hz)	Damping (% Crit.)	Frequency (Hz)	Damping (% Crit.)	Diff (%)	MAC	Description
1	1.00	3.39	0.97	2.66	-3%	96	1st Tower Bending Edgewise
2	1.01	3.82	0.99	2.95	-2%	83	1st Tower Bending Flapwise
3	2.02	2.48	1.88	2.87	-7%	68	1st Blade Flapwise Bending - Asym
4	2.04	2.51	2.00	2.36	-2%	50	1st Blade Flapwise Bending - Asym
5	2.40	2.13	2.37	1.59	-1%	82	1st Blade Flapwise Bending - Sym
6	3.65	1.45					1st Blade Edgewise Bending - Asym
7	3.73	1.24	3.75	0.01	0%	32	1st Blade Edgewise Bending - Asym
8	5.33	1.35	5.05	1.96	-5%	76	2nd Blade Flapwise Bending - Asym
9	5.36	1.46	5.34	1.26	0%	68	2nd Blade Flapwise Bending - Asym
10	6.67	1.20	6.70	0.98	0%	88	2nd Blade Flapwise Bending - Sym
11	7.83	1.38	7.76	1.18	-1%	90	2nd Tower Bending Flapwise
12	7.97	1.19	7.99	1.52	0%	85	2nd Tower Bending Edgewise
13	8.43	1.32	8.34	0.80	-1%	89	1st Tower Torsion, 2nd Blade Edgewise Bending
14	9.67	1.65	9.99	1.64	3%	73	2nd Blade Edgewise Bending - Sym
15	11.15	1.19	11.12	1.29	0%	83	3rd Blade Flapwise Bending - Asym
16	12.52	3.64					3rd Blade Flapwise Bending - Asym
17	12.69	1.70	12.17	2.68	-4%	84	2nd Blade Edgewise Bending - Asym / 3rd Blade Flap - Asym
18	13.45	1.06	13.22	1.11	-2%	71	2nd Blade Edgewise Bending - Asym
19	13.66	1.08	13.82	1.98	1%	66	2nd Blade Edgewise Bending - Asym / 3rd Blade Flap -Sym
20	13.80	1.04					3rd Blade Flapwise Bending -Sym

Using wind as natural excitation to the turbine with the rotors parked, operational modal analysis was performed to extract modal parameters. The same instrumentation set used for the impact modal survey was used to collect time histories during the day, when wind speeds were at approximately 14 m/s. During this testing, the rotors were parked approximately parallel to the wind direction, which allowed for better excitation of the edgewise bending modes. Approximately two hours of continuous data was measured for the operational modal extraction. Figure 7 provides some example time histories for instrumentation on the blades, showing sufficient excitation.

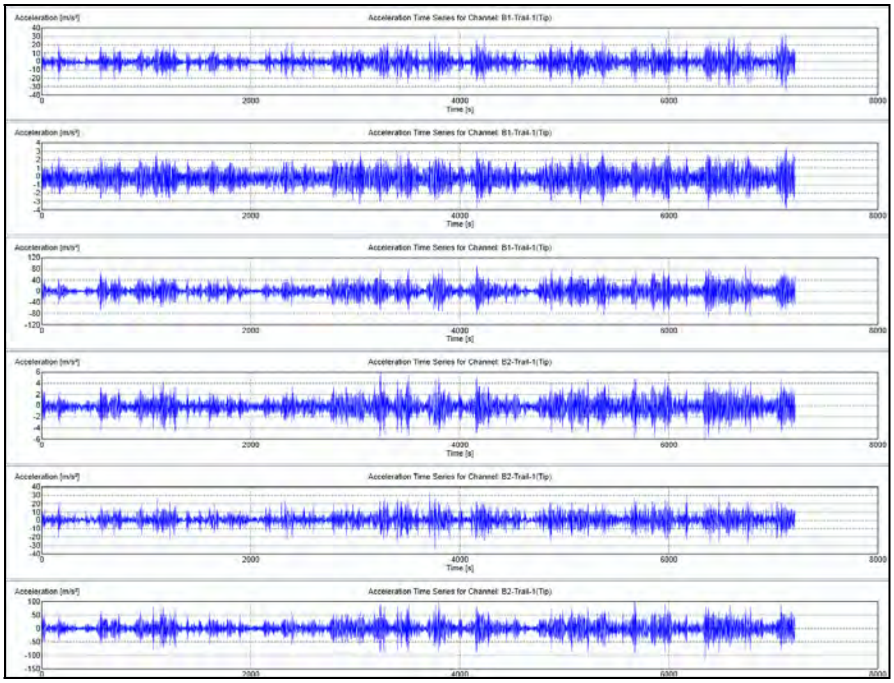

Figure 7. Example time histories collected using natural wind excitation.

The time histories recorded on SNL1 were then used in Structural Vibration Solutions' ARTeMIS software. ARTeMIS has several modal parameter extraction algorithms, which were all investigated with the data. The Crystal Clear Canonical Variate Analysis Stochastic Subspace Identification (SSI-CVA) and the Crystal Clear Unweighted Principal Components Stochastic Subspace Identification (SSI-UPC) were shown to extract a significantly greater number of modes than the other SSI and FDD algorithms available. In the 0–15 Hz frequency band of interest, eighteen modes were extracted with the SSI-CVA and twenty-two modes were extracted with the SSI-UPC algorithm. The stability diagram for the Crystal Clear SSI-CVA algorithm is shown in Figure 8, and the stability diagram for the Crystal Clear SSI-UPC is shown in Figure 9.

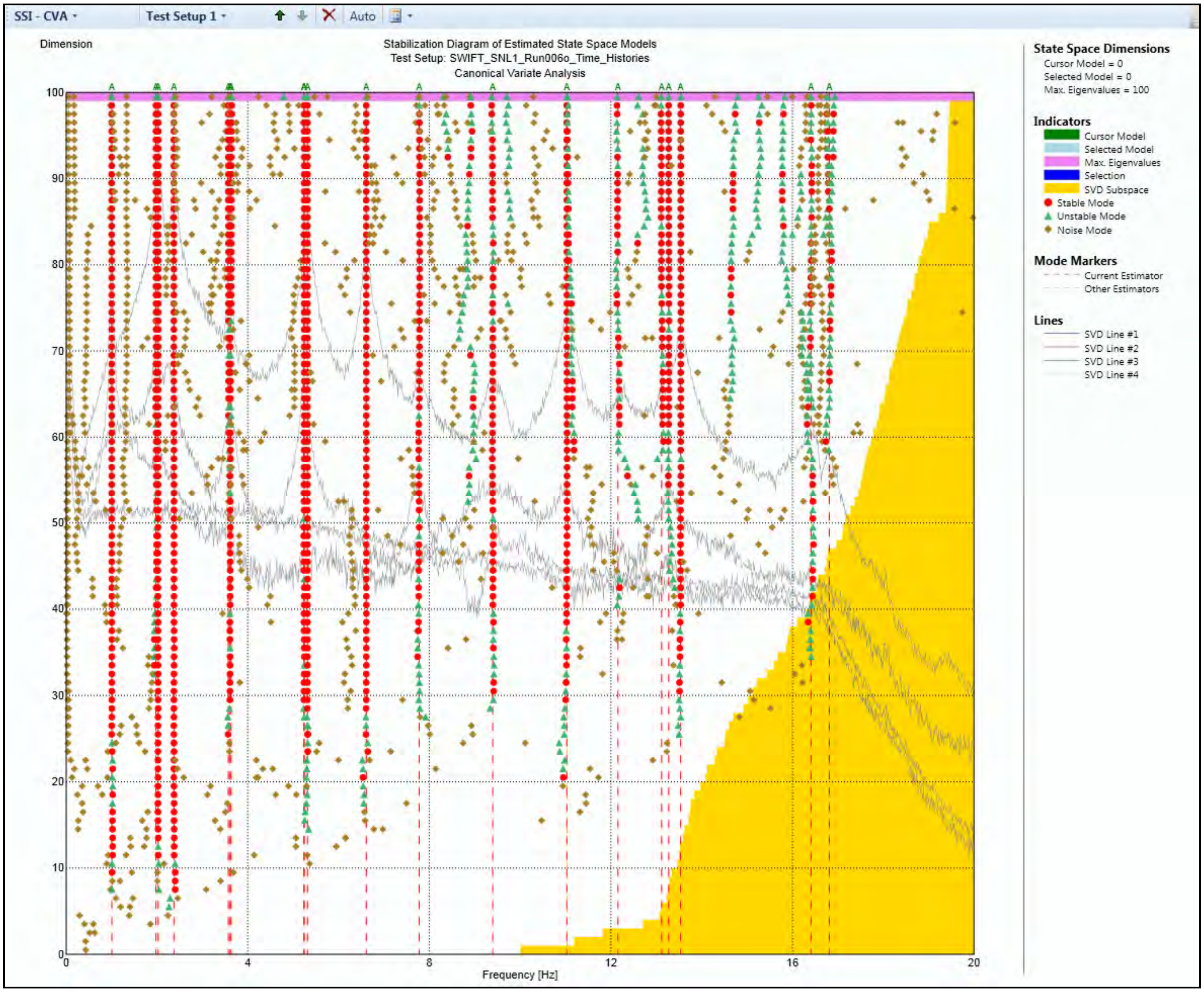

Figure 8. Stability diagram in ARTeMIS for the SSI-CVA algorithm.

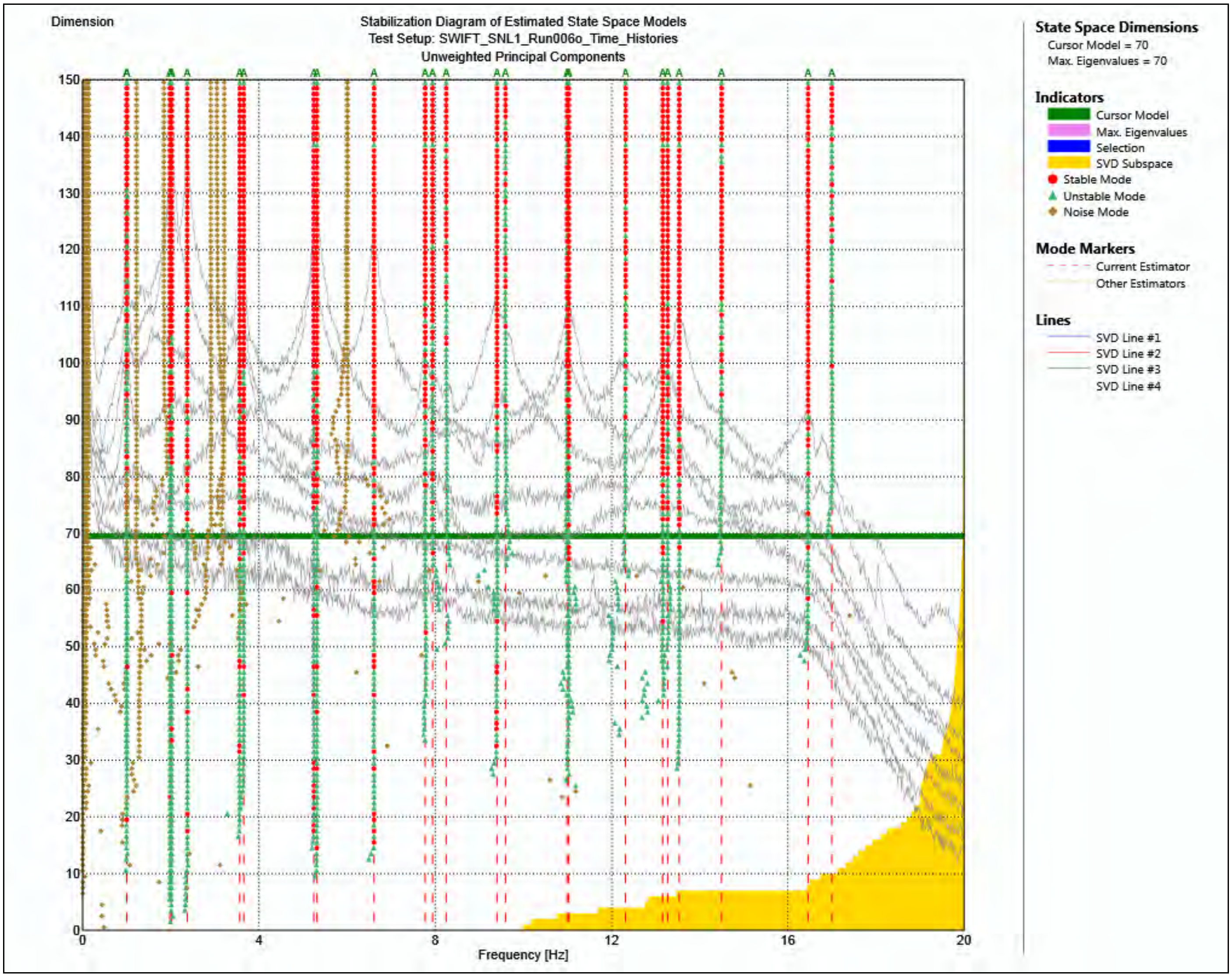

Figure 9. Stability diagram in ARTeMIS for the SSI-UPC algorithm.

A MAC was used to compare the modes extracted using OMA to the EMA-extracted modes. Out of the all the modes extracted in ARTeMIS, eighteen modes correlated to the EMA modes. Table 2 lists the comparisons between the EMA and OMA results on SNL1 and shows that none of the eighteen modes correlated had a frequency difference greater than 3%. In addition, several of the modes correlated had damping differences of less than 20%, indicating very high-quality modal parameters estimated with both techniques. While the SSI-CVA and SSI-UPC yielded similar results, the best set was compiled for the final comparison between EMA and OMA.

The first two tower bending modes have poor MAC values between the EMA and OMA shape. These modes were visually examined and determined to be similar, though bending in slightly different directions and accordingly yielding poor MAC values. The complete MAC table between the EMA and OMA is provided in Table 3.

Table 2. Mode comparisons between EMA and OMA of SNL1.

	SNL1 - EMA		SNL1 - OMA						
Mode	Frequency (Hz)	Damping (% Crit.)	Frequency (Hz)	Damping (% Crit.)	OMA Algorithm	Frequency Diff (%)	Damping Diff (%)	MAC	Description
1	1.00	3.39	1.00	0.90	UPC	-1%	-116%	51	1st Tower Bending Edgewise
2	1.01	3.82	1.00	0.14	UPC	0%	-186%	64	1st Tower Bending Flapwise
3	2.02	2.48	1.98	2.73	CVA	-2%	10%	85	1st Blade Flapwise Bending - Asym
4	2.04	2.51	2.02	2.33	CVA	-1%	-8%	98	1st Blade Flapwise Bending - Asym
5	2.40	2.13	2.37	1.89	CVA	-1%	-12%	100	1st Blade Flapwise Bending - Sym
6	3.65	1.45	3.57	1.02	CVA	-2%	-35%	96	1st Blade Edgewise Bending - Asym
7	3.73	1.24	3.65	0.79	UPC	-2%	-44%	97	1st Blade Edgewise Bending - Asym
8	5.33	1.35	5.24	1.43	CVA	-2%	5%	92	2nd Blade Flapwise Bending - Asym
9	5.36	1.46	5.32	1.27	CVA	-1%	-14%	94	2nd Blade Flapwise Bending - Asym
10	6.67	1.20	6.61	1.04	CVA	-1%	-14%	100	2nd Blade Flapwise Bending - Sym
11	7.83	1.38	7.78	1.27	CVA	-1%	-8%	99	2nd Tower Bending Flapwise
12	7.97	1.19	7.94	1.11	UPC	0%	-7%	78	2nd Tower Bending Edgewise
13	8.43	1.32	8.25	1.95	UPC	-2%	39%	95	1st Tower Torsion, 2nd Blade Edgewise Bending
14	9.67	1.65	9.40	2.09	CVA	-3%	23%	96	2nd Blade Edgewise Bending - Sym
15	11.15	1.19	11.03	1.14	CVA	-1%	-4%	100	3rd Blade Flapwise Bending - Asym
16	12.52	3.64							3rd Blade Flapwise Bending - Asym
17	12.69	1.70	12.32	3.44	UPC	-3%	68%	91	2nd Blade Edgewise Bending - Asym / 3rd Blade Flap - Asym
18	13.45	1.06	13.12	1.08	CVA	-3%	1%	98	2nd Blade Edgewise Bending - Asym
19	13.66	1.08							2nd Blade Edgewise Bending - Asym / 3rd Blade Flap -Sym
20	13.80	1.04	13.54	1.11	CVA	-2%	6%	97	3rd Blade Flapwise Bending -Sym

Table 3. MAC comparing modes between EMA and OMA on SNL1.

EMA/OMA Cross MAC Table

EMA Shapes

OMA Shapes		1	2	3	4	5	6	7	8	9	10	11	12	13	14	15	16	17	18	19	20
	MAC	1.00	1.01	2.02	2.04	2.40	3.65	3.73	5.33	5.36	6.67	7.83	7.97	8.43	9.67	11.15	12.52	12.69	13.45	13.66	13.80
1	1.00	0.51				0.26															
2	1.00		0.64			0.43															
3	1.98			0.85						0.24				0.25			0.25	0.22			
4	2.02			0.41	0.98				0.22	0.47		0.25				0.34					
5	2.37		0.23			1.00					0.54									0.21	0.26
6	3.57						0.96												0.25		
7	3.65							0.97													
8	5.24								0.92			0.36		0.46				0.41			
9	5.32			0.32	0.51				0.21	0.94		0.43				0.55	0.24				
10	6.61					0.54					1.00									0.44	0.54
11	7.78				0.31				0.51	0.30		0.99				0.64					
12	7.94												0.78								
13	8.25			0.21					0.21	0.27				0.95			0.54	0.32			
14	9.40														0.96						
15	11.03				0.36				0.31	0.42		0.61				1.00					
16	12.32								0.23					0.47			0.85	0.91			
17	13.12						0.26												0.98		
18	13.54					0.28					0.58									0.80	0.97

Using OMA to obtain modal properties of large structures such as wind turbines has several advantages. Imparting large measured external excitation can be a difficult, time-consuming, and expensive task. In addition, these structures may be in an environment where unmeasured external excitation is significant, making it difficult to take high-quality measurements using traditional modal methods. With the test presented in this paper, natural wind excitation was present, and there was little time when the wind was at a minimal speed acceptable for performing an impact modal survey. The higher wind speeds during the majority of the day made modal testing impossible not only because of the wind excitation producing more response in the structure than the modal impact sledge but also because of safety limitations of using a personnel lift at that height. With OMA, once instrumentation was installed, data collection could happen over the course of several hours to several days with minimal support.

SUMMARY

ATA Engineering was contracted by SNL to perform modal testing on components and assemblies of two Vestas V27 wind turbines at the SWiFT facility in Lubbock, Texas. Modal testing was performed on two full turbines, and frequencies, damping, and shapes were shown to correlate, although with minor differences between the turbines. This paper also demonstrated that natural wind excitation is sufficient to excite the majority of modes of a parked V27 wind turbine up to 15 Hz. Using SVS's ARTeMIS software, eighteen modes were highly correlated to the experimental modal results on the SNL1 turbine.

REFERENCES

[1] G.H. James, T.G. Carne, J.P. Lauffer, and A.R. Nord, "Modal Testing Using Natural Excitation," *Proceedings of the 10th International Modal Analysis Conference* (IMAC), San Diego, California, 1992, pp. 1209–1216.

[2] T.G. Carne and G.H. James, "The Inception of OMA in the Development of Modal Testing Technology for Wind Turbines," *Mechanical Systems and Signal Processing* 24, pp. 1213–1226, 2010.

[3] R. Brinker, P. Andersen, and L. Zhang, "Modal Identification from Ambient Responses Using Frequency Domain Decomposition," *Proceedings of The 18th International Modal Analysis Conference* (IMAC), San Antonio, Texas, 2000, pp. 625–630.

[4] R. Brinker, L. Zhang, and P. Andersen, "Modal Identification of Output-Only Systems Using Frequency Domain Decomposition," *Smart Materials and Structures* 10, pp. 441–445, 2001.